A new morphotype description of Arbacia spatuligera Valenciennes, 1846 (Arbacioida, Echinoidea) and bathymetric range extension from mesophotic reefs of the central coast of Chile.

Rigoberto Moreno-Mendoza, Erwan Courville, Luis Enrique Angeles-Gonzalez, Julio Duarte, Marc Carulla, Daniel Malfanti-Bravo, Andrés Mena-Auladell, Thomas Saucède, Nuno Simões, Elie Poulin

To cite this version:

Rigoberto Moreno-Mendoza, Erwan Courville, Luis Enrique Angeles-Gonzalez, Julio Duarte, Marc Carulla, et al.. A new morphotype description of Arbacia spatuligera Valenciennes, 1846 (Arbacioida, Echinoidea) and bathymetric range extension from mesophotic reefs of the central coast of Chile.. Journal of the Marine Biological Association of the United Kingdom, 2024, 104, pp.e48. ⟨10.1017/S0025315424000389⟩. ⟨hal-04596433⟩

HAL Id: hal-04596433
https://ube.hal.science/hal-04596433v1

Submitted on 18 Feb 2025

A NEW MORPHOTYPE DESCRIPTION OF ARBACIA SPATULIGERA VALENCIENNES, 1846 (ARBACIOIDA, ECHINOIDEA) AND BATHYMETRIC RANGE EXTENSION FROM MESOPHOTIC REEFS OF THE CENTRAL COAST OF CHILE

Journal:	*Journal of the Marine Biological Association of the United Kingdom*
Manuscript ID	JMBA-08-23-0136
Manuscript Type:	Research Article
Date Submitted by the Author:	28-Aug-2023
Complete List of Authors:	Moreno-Mendoza, Rigoberto; Universidad Catolica de la Santisima Concepcion - Campus San Andres, Facultad de Ciencias Courville, Erwan; Biogéosciences, UMR 6282 CNRS, Université de Bourgogne Ángeles–González, Luis ; Universidad Nacional Autónoma de México. Sisal, Yucatán, C.P. 97356, México Duarte, Julio; Centro de Investigación y de Estudios Avanzados del Instituto Politécnico Nacional (Cinvestav), Unidad Mérida. Km. 6. Antigua carretera a Progreso, Mérida, México Carulla, Marc; Tamarugo Dive Center Malfanti-Bravo, Daniel; Tamarugo Dive Center Mena-Auladell, Andres; 7. Vicerrectoría de Finanzas, Departamento TI, Universidad de las Américas, Manuel Montt 948 Saucède, Thomas; Biogéosciences, UMR 6282 CNRS, Université de Bourgogne Simões, Nuno; Universidad Nacional Autonoma de Mexico, UMDI-Sisal, PIECEMO; Poulin, Elie; Instituto Milenio de Ecosistemas Antárticos y Subantárticos (BASE); Universidad de Chile Facultad de Ciencias
Keywords:	echinodermata, biodiversity, rocky reef, rebreather diving, scientific diving
Abstract:	The sea urchin Arbacia spatuligera is an echinoid distributed in the Southeastern Pacific Ocean from Peru to Chile. This species was previously reported from the subtidal zone with a bathymetric distribution up to 30 m depth. In this work, 128 individuals were found in four mesophotic reefs along the central coast off Chile using Closed Circuit Rebreathers in technical diving at higher depths than previously, ranging from 36 to 63 meters in depth. A population exhibits unexpected morphological characters, requiring an emended diagnosis and description of a new morphotype for A. spatuligera. These morphological traits are further discussed as potential ecophenotypic adaptations.

A NEW MORPHOTYPE DESCRIPTION OF *ARBACIA SPATULIGERA* VALENCIENNES, 1846 (ARBACIOIDA, ECHINOIDEA) AND BATHYMETRIC RANGE EXTENSION FROM MESOPHOTIC REEFS OF THE CENTRAL COAST OF CHILE

A NEW MORPHOTYPE OF *A. SPATULIGERA* IN MESOPHOTIC REEFS

Rigoberto Moreno-Mendoza[1,2], Erwan Courville[3,4], Luis Enrique Ángeles-González[5], Julio Duarte[6], Marc Carulla[2], Daniel Malfanti-Bravo[2], Andrés Mena-Auladell[2,7], Thomas Saucède[3], Nuno Simões[5] & Elie Poulin[4]

1. Doctorado en Ciencias con mención en Biodiversidad y Biorecursos, Facultad de Ciencias, Universidad Católica de la Santísima Concepción, Av. Alonso de Ribera 2850, Concepción, Chile. Email: rmoreno@doctorado.ucsc.cl
2. Tamarugo Dive Center, Av. Blanca Estela 1927, Local 16, Concón, Chile.
3. Biogéosciences, UMR 6282 CNRS, Université de Bourgogne, 6 Boulevard Gabriel, 21000, Dijon, France.
4. Instituto Milenio de Ecosistemas Antárticos y Subantárticos (BASE) and Facultad de Ciencias, Universidad de Chile, Santiago, Chile
5. Unidad Académica Sisal, Facultad de Ciencias, Universidad Nacional Autónoma de México, Puerto de Abrigo s/n, C.P. 97356, Sisal, México.
6. Centro de Investigación y de Estudios Avanzados del Instituto Politécnico Nacional (Cinvestav), Unidad Mérida. Km. 6. Antigua carretera a Progreso, Mérida, México.
7. Vicerrectoría de Finanzas, Departamento TI, Universidad de las Américas, Manuel Montt 948, Santiago, Chile.

Abstract

The sea urchin *Arbacia spatuligera* is an echinoid distributed in the Southeastern Pacific Ocean from Peru to Chile. This species was previously reported from the subtidal zone with a bathymetric distribution up to 30 m depth. In this work, 128 individuals were found in four mesophotic reefs along the central coast off Chile using Closed Circuit Rebreathers in technical diving at higher depths than previously, ranging from 36 to 63 meters in depth. A population exhibits unexpected morphological characters, requiring an emended diagnosis and description of a new morphotype for *A. spatuligera*. These morphological traits are further discussed as potential ecophenotypic adaptations.

Keywords: echinodermata, biodiversity, rocky reef, rebreather diving, scientific diving

Introduction

Sea urchins form a large group of benthic marine invertebrates belonging to the phylum Echinodermata, which comprises approximately 1,000 valid species belonging to 115 genera (Mickael et al., 2016; Luparello et al., 2020), distributed at all latitudes in various marine environments and ranging from the intertidal to the deep sea (Iken et al., 2001; Lebrato et al., 2010). The order Arbacioida Gregory, 1900 includes 26 known extant species and eight recognized genera belonging to a single family, the Arbaciidae Gray, 1855. Within the family, the genus *Arbacia* Gray, 1835 is distributed from tropical to temperate and sub-Antarctic regions of the Pacific, Atlantic oceans, and Mediterranean Sea and comprises five valid species: *Arbacia dufresnii* (Blainville, 1825*)*, *Arbacia lixula* (Linné, 1758), *Arbacia punctulata* (Lamarck, 1816), *Arbacia spatuligera* (Valenciennes, 1846), and *Arbacia stellata* (Blainville, 1825) (Gianguzza & Bonaviri, 2013).

The species *A. spatuligera* is located in the Southeastern Pacific Ocean from northern Peru to Puerto Montt, in south-central Chile (Larraín, 1975; Lessios et al., 2012; Millán et al., 2019). Valenciennes first described the species in 1846 with reliable and detailed drawings and descriptions for that time. More recent descriptions and figures were published by Koehler (1914). In 1935, Mortensen mentioned that the species easily distinguished from the other southern species *Arbacia dufresnii* by its color, with "no green (patches of) nor red color in the interambulacral – as also by its club-shaped aboral spines". Larraín (1975) defined neotypes for *Arbacia spatuligera* in an extensive monography focused on extant and fossil echinoid species from Chile. He proposed a new detailed description of the species and an extended diagnosis.

Bathymetric records of *A. spatuligera* indicate that the species occurs in shallow waters above 30 m depth (Larraín, 1975; Lessios et al., 2012; Gianguzza & Bonaviri, 2013; Millán et al., 2019). However, due to logistical limitations to recreational scuba diving, most of the knowledge about the distribution and ecology of *A. spatuligera* was based on information obtained from shallow areas (<30 m depth) (Kramer et al., 2019).

Mesophotic Reef Ecosystems (MREs) are considered a continuation of shallow reefs (Hinderstein et al., 2010) with depths up to 150 m in tropical and subtropical latitudes (Rocha et al., 2018). They are characterized by the presence of light-dependent organisms and their associated biological communities (Eyal & Pinheiro, 2020). Along the central coast of Chile, Temperate Mesophotic Reef Ecosystems (TMRE) have been poorly studied due to the logistic implications of taking samples in zones that exceed the no-decompression limits for recreational scuba diving (Shreeves & Richardson, 2006). These logistic limitations are reflected in the little information available about species' bathymetric ranges, habitat preferences, and communities' structures (Kahng et al., 2010). In order to explore and generate new knowledge about these deep ecosystems, technical dives with Closed-Circuit Rebreathers (CCRs) were performed for the first time over Chilean temperate reefs. As a result, the present work presents novel ecological information about the presence and distribution of the sea urchin *A. spatuligera* in four temperate mesophotic reef ecosystems of the continental shelf off Chile, in addition to data from two shallow rocky reefs.

Material & Methods

In February 2019, April, May, August, and September 2022, photographic and video records of the sea urchin *Arbacia spatuligera* were obtained from four mesophotic rocky reefs: Pichidangui in the Coquimbo Region, two artificial reefs (shipwrecks), and one sandy slope at Valparaíso Bay, between 36 and 63 m depth, nearby the central coast off Chile (Figure 1). 30-minute bottom time dives were performed to search for the target species. Photos and videos were taken using a GoPro 9 and a Sony RX100 V camera with underwater housing and a light system. A Shearwater Petrel dive computer recorded the depth at which organisms were observed. All dives were made during the day using the JJ-CCR rebreather with different gas mixtures as diluents (air and trimix) according to the maximum depth for each dive (Table I).

We recorded 128 individuals of *Arbacia spatuligera* in four mesophotic reefs on the central coast of Chile at depths ranging between 36 and 63 m. (Table I). The four reefs presented differences in habitat and light conditions. Large rocks with filamentous algae (turf), sponges, crustose algae (order Corallinales), and channels with sand characterized the rocky reef of Pichidangui. Both wrecks in the Bay of Valparaíso lie on a bottom of fine sand and silt with filamentous algae and the striped anemone *Anthothoe chilensis* (Lesson, 1830) attached to the deck and hull. Light penetration at both sites is limited compared to the Pichidangui rocky reef. The sandy slope presented much plastic debris and abandoned fishing gear, which was used as a substrate for individuals of *A. spatuligera*. On this site, three individuals of *A. spatuligera* were observed next to three specimens of the lobed anemone *Antholoba achates* (Drayton, 1846). The highest abundance of this species was recorded in the rocky reef of Pichidangui at depth ranges between 40-58 m. On this site, we found variable numbers ranging from a single individual to an aggregation of 11 sea urchins on the rocky substrate (Figure 2). The artificial reef with the lowest abundance (10 individuals) was the deepest wreck at 63 m. The organisms with the smallest recorded size were found on the sandy slope with debris, while the organisms with the largest sizes were observed on the rocky reef of Pichidangui.

Twelve individuals were collected at 53 meters' depth off Pichidangui (Figure 1) for specimen identification in May 2023. The collected specimens exhibit striking similarities in all aspects to those photographed during the initial fieldwork in 2022 (Fig. 2I-O). Samples were preserved in 95% ethanol and prepared for morphological observations and DNA sequencing. To perform morphological observations, tests were cleaned off using a brush and a diluted bleach solution, allowing removal of all spines and soft tissues to reveal the plate patterns. Systematic nomenclature and terminology for morphological description follow Kroh (2020). Plates are numbered according to Lovén's system (Lovén, 1874).

The isolation of DNA, PCR, and preparation for Sanger sequencing were performed in the Molecular Ecology Laboratory of the Millennium Institute of Biodiversity of Antarctic and Subantarctic Ecosystems at Universidad de Chile, Chile. DNA was extracted from the spines and gonads preserved in 95% ethanol using the Dneasy Blood & Tissue Kit by QIAGEN. The mitochondrial genome's Cytochrome Oxydase subunit I (COI) was amplified for seven individuals. COI primers specific to the genus *Arbacia* were used, ArbaF and ArbaR (Haye et al., 2014). PCR's were performed using Accustart II PCR ToughMix (ref. 95142-800) following notice volumes (for a 50 µl PCR reaction, 5 µl of total genomic DNA, 1 µl of each primer and 25 µl of Taq polymerase). Cycling conditions consisted of an initial denaturation at 94°C for 3 min followed by 40 cycles of 1 min denaturing at 94°C, 45 sec annealing at 45°C, and a 1 min extension at 72°C., with a final 3min extension at 72°. Sequencing was performed in one direction using automatic sequencers from MACROGEN Chile.

Results

Genetic data. All seven specimens sequenced from Pichidangui correspond to one unique COI haplotype of *Arbacia spatuligera*, already recorded by Millán et al. (2019). The haplotype sequence was deposited in the GenBank database (GenBank accession member requested). It corresponds to the COI haplotype "AspaCN1" (GenBank accession number: MK382495.1), and this haplotype corresponds to the Hap1 on the haplotype network presented by Millán et al. (2019) and aligns with the most prevalent haplotype (114 out of 140 individuals; Millán et al., 2019) within *A. spatuligera*, found from Concepción (Chile) to Lima (Peru) in shallow water (0-30 m).

Morphological data. The specimens observed along the coasts of Valparaiso (Fig. 2A-H) exhibit the typical morphology of *Arbacia spatuligera* as described by Mortensen (1935) and Larraín (1975): they are characterized by white, short, and club-shaped spines on the aboral side and long, and slender spines at the ambitus. The test coloration is light brown, and the interambulacrum is marked by a vestigial bare interambulacral area in larger specimens, in accordance with previous descriptions by Mortensen (1935) and Larraín (1975). In contrast, samples from Pichidangui (Fig. 2I-O) were distinguished by long and slender dark brown spines extending adapically along the interambulacrum up to the apical system. The test coloration in these specimens is dark green, which deviates from the typical light brown to light green coloration observed in other studied specimens.

The morphological study of specimens from Pichidangui enabled the identification of diagnostic characters of the species *A. spatuligera* (Fig. 3A-C) as described by Mortensen (1935) and Larraín (1975). It includes a narrow naked interambulacral area reduced to the interradius in larger specimens (Figure 3C), poorly developed aboral ambulacral tubercles that do not reach the ocular plates (Figure 3A), supra-anal plates forming a pyramid shape with small and narrow extensions at the tips (Figure 3A), and larger ambulacral pores compared to other species of the genus (Figure 3C). However, specimens from Pichidangui also show unique morphological characters that had been not reported in *Arbacia spatuligera* so far (Valenciennes, 1846; Koehler, 1914; Lovén, 1887; Mortensen, 1910, 1935; L. Agassiz & Desor, 1846; A. Agassiz, 1872; A. Agassiz & Clark, 1908). Interambulacral tubercles are large, with usually three tubercles per plate of a subequal size above the ambitus and the same size throughout the aboral surface (Figure 3A, C). The adoral area is characterized by shorter phyllodes and a pentagonal peristome (Figure 3B). This population's tags are much smaller, only reaching the second interambulacral plate (Figure 3B). The aboral spines are brown, long and slender, even close to the apical system, and the test shows an overall dark green coloration (Figure 2I-O). These morphological variations have prompted the need for an amended diagnosis to describe and characterize *A. spatuligera* accurately.

Systematic part

Phylum Echinodermata Klein, 1778

Class Echinoidea Schumacher, 1817

Order Arbacioida Gregory, 1900

Family Arbaciidae Gray, 1855

Genus *Arbacia* Gray, 1835

Arbacia spatuligera (Valenciennes, 1846)

1846 *Echinus* (*Agarites*) *spatuligera* Agassiz & Desor: p. 353.

1872 *Arbacia spatuligera* A. Agassiz: p. 93; p. 403, pl. 35, fig 7.

1912 *Arbacia spatuligera* Jackson: p. 115; p. 158.

1914 *Arbacia spatuligera* Koehler: p. 240; pl. 12, figs. 14;19–20.

1935 *Arbacia spatuligera* Mortensen: p. 577–579; pl. 70, figs 1–5; pl. 71, fig 6; pl. 87, figs 1–6.

Emended diagnosis. *Arbacia* with ambulacral tubercles not reaching the apical system; tip of supra-anal plates with a small and narrow extension; extended phyllodes, resulting in a highly intricate contour of the peristome; interambulacral bare area vestigial in the largest specimens (D> 65 mm); color brown to green; spines white to light brown.

Type material. Type specimen never established. Larraín (1975) defined a neotype, housed in the Museum of the Zoological Department of the Universidad de Concepción, Chile under reference number 7966.

Occurrence. *A. spatuligera* is found within the Warm Temperate Southeastern Pacific Province (Spalding et al., 2007), spanning a latitude range from 42° to 6°S between Puerto Montt (south-central Chile) to Chiclayo (northern Peru). Mortensen (1935) mention the presence of *A. spatuligera* in Guayaquil, Ecuador, near 2°S latitude, in the Tropical Eastern Pacific Province. However, none of the specimen preserved in the large, extensive collection of the natural history museum comes from Ecuador and this occurrence remains doubtful.

It was initially reported from the subtidal zone, as documented by Mortensen (1935), Larraín (1975), and Millán et al. (2019). Our study reveals its presence in deeper mesophotic environments as well.

Emended description. Test circular to subpentgonal in outline at ambitus. Test large, reaching 70 to 80 mm in diameter. Living specimens dark brown to dark green, with lighter, usually white, spines. Denuded test light green, sometimes deep brown. Allometric relationship between test height and test diameter described by linear regression model $\ln(y) = 1.05\ln(x) - \ln(0.8554)$; $R^2 = 0.9136$.

Apical system Small, dicyclic to hemicyclic, with no tubercles. Ocular plates usually exsert (53%) in large specimens (TD > 40 mm), plate V often insert (47%) and plates I rarely insert (5%). Plates I and IV closer to periproct margin. Juveniles always with dicyclic apical system, ocular plates becoming insert with growth. Ocular and genitals free of tubercles in adults. Periproct oval with maximum diameter in direction 1-IV, as it is usually the case in species of the genus *Arbacia*. Gonopores small, slightly elongated. Ocular plates with numerous ophicephalous pedicellariae, connected to the plate by a small, circular granule.

Peristome Relative peristome diameter large, usually close to 50% of the test diameter. Buccal notches deep, tags usually long and narrow (spanning up to 3 tubercles), shorter in specimens from Pichidangui (spanning < 2 tubercles). Peristome shape usually characterized by extended phyllodes, resulting in a highly intricate contour of the peristome. Perignathic girdle thin and long, auricles usually not in contact, forming an arch over the perradius. Peristome relative size decreasing with growth. Allometric relationship between peristome diameter and test diameter described by linear regression model $\ln(y) = 0.7088\ln(x) + \ln(0.4042)$; $R^2 = 0.902$.

Ambulacra Narrow (half of the interambulacra), each plate with one imperforate and non-crenulate primary tubercle of the same size as interambulacral ones at the ambitus and quickly decreasing in size adapically. Tubercles spaced aborally, not reaching apical system.

Tubercles separated by fine granules at the perradial suture. Ambulacral plates trigeminate from ambitus to apical system, of arbaciid type aborally, forming more complex compound plating adorally and leading to narrow phyllodes adorally. Aborally, pores of a pair deeply conjugate, and pore-pairs separated by marked ridges. Neural canal poorly developed. Close to peristome, single perradial pit for sphaeridium along perradius of each ambulacrum.

Interambulacra Wide, with up to five imperforate and non-crenulate primary tubercles per plate at the ambitus, all similar in size in large specimens (TD > 70 mm). Smaller specimens (TD < 50 mm) bear three to four tubercles at ambitus. Tubercles decrease in size above the ambitus. Inner tubercles abutting the oral suture of the plate and usually decreasing in size toward interradius, except for specimens from Pichidangui with subequals tubercles aborally (Fig. 3). Adradial column of large primary tubercles reaches the apical system. The second column of tubercles almost reaches the apical system. Tubercles with large mamelons, narrow platforms, and broad areoles, occupying most of plate width at ambitus. Except for naked interradial area, plates coarsely granulated between tubercles. Bare area usually restricted to interradius and vestigial in large specimens (TD > 70 mm). Number of interambulacral plates high, usually between 15-16 plates (TD = 40 mm) and 17 plates (TD = 50 mm). Large specimens, reaching 70 mm TD, bears up to 21 interambulacral plates. Height of plates not varying along aboral surface adapically.

Pedicellariae of three types, ophicephalous, tridentate and triphyllous, abundant over the test. All pedicellariae are white in adult specimens.

Ophicephalous pedicellariae (Fig. 5A, B) differentiated between the oral and aboral sides. Aboral surface covered with numerous ophicephalous pedicellariae, including area surrounding the apical system. Valves of ophicephalous pedicellariae circular, narrow, and constricted in upper part, with indented and sharply serrated blade edges (Fig. 5A). Buccal membrane covered by second type of ophicephalous pedicellariae (Fig. 5B) with higher, elongated valves, indented blade edges, and slight serration. Upper part of the valve slightly constricted.

Tridentate pedicellariae (Fig. 5C-D) small, being only twice as long as ophicephalous pedicellariae. Abundant on both oral and aboral surface, including on ocular plates but absent on buccal membrane. Valves of tridentate pedicellariae slender, elongated, and not constricted in the middle. Blade edges finely serrated. Width-to-length ratio varies between 0.51 and 0.63 (Fig. 5C-D).

Triphyllous pedicellariae scarce and resemble those found in other *Arbacia* species, as noted by A. Agassiz & Clark (1908) and Larraín (1975). Valves of triphyllous pedicellariae elongated and constricted in middle part. Blade edges finely serrated.

Spines Two morphologies of *A. spatuligera* spines are known. Typical form with aboral spines short and robust, exhibiting a distinctive "club-shaped" morphology (Mortensen, 1935); long, and slender at ambitus. Spines length usually equal to test diameter, up to 50 mm. Specimens from Pichidangui with long and slender spines over the entire aboral side, up to apical system. Presence of long and sturdy aboral spines, consistently sized across the aboral surface, linked to the presence of large, equally sized interambulacral tubercles. Ambital and subambital spines with large "enameled" tips. Spines white in typical form, but appear darker, approaching a brown hue in long-spine form.

Remarks. The presence of a well-developed epistroma, of sphaeridiae positioned in adoral pits in each perradius, of imperforate and non-crenulate tubercules, and of a periproct with four anal plates support the assignment of the species to the order Arbacioida. The compound, arbaciid-like plates of ambulacra, the occurrence of tubercles similar in size in both ambulacra and interambulacra at the ambitus, and of a clear difference in tuberculation between the oral and aboral side (aboral tubercles highly reduced in size and number), are diagnostic of the family Arbaciidae. The presence of a straight pore-zone with tube feet not arranged into in arcs of three, of ambulacral tubercles forming a regular series throughout, of a large peristome (> 30% of test diameter), of interambulacra with numerous primary tubercles arranged in horizontal and vertical series, of a single sphaeridial pit near the peristomial edge in each interambulacrum, and of straight and finely striated spines with an enameled tip are all diagnostic characters of the genus *Arbacia*.

Discussion

Specimens of *A. spatuligera* from Pichidangui depart from the typical morphology of the species formerly described (Mortensen 1935, Larraín 1975), which raises questions about the underlying processes at play. These morphological variations have prompted the need for an amended diagnosis to describe and characterize A. spatuligera accurately. The absence of genetic difference in COI gene between the two morphotypes suggests that morphological differences observed between the specimens from Pichidangui and the typical form are not the result of a genetic differentiation linked to either geographic isolation or ecological niche evolution in deeper environments. Millán et al. (2019) emphasized the absence of genetic structure and unexpectedly low genetic diversity in populations of *A. spatuligera* over its entire distribution range. Additionally, they found evidence of a recent demographic expansion of the species, estimated to have occurred 33,000 to 47,000 years ago. This is in line with the unique haplotype found in the studied specimens and the absence of genetic difference identified in COI sequences between the two morphologies.

The observed morphological variations may also result from phenotypic plasticity. The differences in spine length and color are typical of ecophenotypic variations observed in echinoids. Phenotypic plasticity could be defined as the environmental sensitivity of a genotype to produce alternative phenotypes in response to environmental cues (Fusco & Minelli, 2010). Environmental conditions, particularly water currents, frequently influence spine length. The occurrence of the studied specimens in a deep and calm environment with reduced tidal influence may have favored the long spine morphology. The size and density of spines could also play a significant role in providing protection against predators (Smith, 1980). The presence of long and sturdy aboral spines, with large, equally sized interambulacral tubercles, can be readily explained by the necessity of these spines to have a substantial, large muscle surface area for attachment (Smith, 1980). The quantity of oral tube feet significantly impacts the ability to adhere to the substrate, and the observed reduction in the size of phyllodes in specimens from Pichidangui in a low-energy environment aligns with the ecophenotypic interpretation.

It is important to note that a population of *A. spatuligera* with a "typical morphology" has also been observed in mesophotic environments along the coasts of Valparaiso (Fig. 2A-H) at the same depth as those of Pichidangui. Moreover, another specimen, in all aspects similar to those from Pichidangui, was observed at 60 m depth in Algarrobo, Chile (Fig. 7), 200 km away to the south (NUTME 2023 per.com.). Subsequent investigations focusing on the environmental conditions of these specimens, as well as their ecology, coupled with additional genetic studies, will offer further insights into which of these two hypotheses takes precedence.

The bathymetric distribution and habitat preference of the genus *Arbacia* widely varies depending on the species. For instance, the Atlantic purple sea urchin (*Arbacia punctulata*) is located at a maximum depth of 255 m (Hill & Lawrence, 2003) while *A. lixula* is well adapted to shallow waters of the upper infralittoral in the Mediterranean Sea and Madeira Island (Roma et al., 2021). On the other hand, the green sea urchin *Arbacia dufresnii* located from the Pacific Ocean from Puerto Montt (locality where the distribution area of *A. spatuligera* ends) to the Falkland Islands (Bernasconi, 1966) has the deepest distribution of the genus reaching depths of 315 m (Bernasconi, 1953).

The present study extends the known bathymetric range of *A. spatuligera* from 30 to 63 m depth, which is within the range of other species of the genus. No data on the species' density and preferred habitat were available so far. We report that the number of individuals present in each mesophotic reef is low compared to shallow sites in other locations on the Chilean coast (Table I). For example, in the Biobio region, located ~556 km away from our study area, we have recorded up to 220 individuals in Penco and 188 organisms in Laraquete (pers. obs.); both localities do not exceed 8 m depth. Habitat preference in shallow locations was consistent with the presence of a rocky bottom and holdfast and blades of giant kelp (*Macrosystis pyrifera*) and co-occurrence with the black sea urchin *Tetrapygus niger* and the red sea urchin *Loxechinus albus* (Fig. 6).

The abundance of *T. niger* in Penco was lower (55 individuals) than *A. spatuligera*. In the locality of Laraquete, *A. spatuligera* co-occurred with two species of sea urchins, *T. niger* (36 individuals) and *L. albus* with 12 individuals (Fig. 6). In this last locality, individuals of

A. spatuligera were also found in beds of the Magellan mussel (*Aulacomya atra*) (Molina, 1782).

Conclusions

The population found off the coast of Pichidangui (Chile) shows a different morphology compared to all other specimens despite the lack of COI sequence divergence. This allows us to amend the diagnosis and description of the species and discuss these variations as potential ecophenotypic adaptation or recent geographical isolation. *Arbacia spatuligera* has a bathymetric distribution ranging from 5 to 63 m in depth. The species can be found on various bottom types, from rocky reefs with kelps *Macrocystis pyrifera* and *Lessonia* spp., filamentous algae, beds of the bivalve *Aulacomya atra*, to artificial reefs such as shipwrecks and sandy bottoms with hard substrate. It is necessary to continue with studies in this species to determine if there are differences between the feeding habits in shallow and mesophotic organisms. Finally, technical diving using Closed Circuit Rebreathers (CCRs) is a fundamental tool in scientific diving for generating novel ecological knowledge in deep zones below 30 m depth, the recreational diving limit.

Acknowledgements

We thank the two anonymous reviewers for carefully reading our manuscript and their many insightful comments and suggestions. We thank Alder Carrillo for the photos of *Arbacia spatuligera* of Penco and Laraquete.

Author contributions

Rigoberto Moreno-Mendoza: Work conception, data acquisition, analyses, data interpretation, manuscript draft. Erwan Courville: taxonomic identification molecular data acquisition, photography, manuscript draft. Luis Angeles Gonzalez: analyses, data interpretation, manuscript draft. Julio Duarte-Gutierrez: conception, analyses, data interpretation, manuscript draft. Marc Carulla: data acquisition, photography, manuscript draft. Daniel Malfanti-Bravo: conception, data acquisition, manuscript draft. Andrés Mena-Auladell: data acquisition, manuscript draft. Elie Poulin: molecular data acquisition, manuscript draft. Thomas Saucède: taxonomic identification, manuscript draft. Nuno Simões: data acquisition, analyses, data interpretation, manuscript draft.

Financial support

Thanks are due to BIOGEOSCIENCES, Millennium Institute BASE ICN2021_002 and ECOS-ANID ECOS220008. This research is also the product of a postdoctoral fellowship by CONACYT granted to Luis Enrique Ángeles González with CVU 475262 at Centro de Investigación Científica y de Educación Superior de Ensenada, Baja California (CICESE).

Conflict of interest

The authors declare none.

Ethical standards

Does not apply

References

Agassiz A (1872) *Revision of the Echini. Illustrated Catalogue of the Museum of Comparative 354 Zoölogy at Harvard College*. Cambridge [Mass.]: University Press.

Agassiz A and Clark HL (1908) *Hawaiian and other Pacific Echini. The Salenidae, Arbaciadae, Aspidodiadematidae, and Diadematidae*. Cambridge: Printed for the Museum.

Agassiz JLR and Desor PJÉ (1846) Catalogue Raisonné of the Families, Genera and Species of the Class of Echinoderms: A translation of Agassiz, Louis, Desor, E. 1846. Catalogue raisonné des familles des genres et des espèces de la Classe de Echinodermes. Annales des sciences naturelles*. Herizos Press, Tampa* **6**, 305–374.

Bernasconi IM (1953) Monografía de los equinoideos argentinos. *Anales Museo Historia Natural de Montevideo* **6**, 23-25.

Bernasconi IM (1966) Los equinoideos y asteroideos colectados por el buque oceanografico R/V" Vema", frente a las costas Argentinas, Uruguayas y sur de Chile. *Coni*.

Blainville H-MD (1825) *Manuel de malacologie et de conchyliologie*. Paris: F. G. Levrault.

Eyal G and Pinheiro HT (2020) Mesophotic ecosystems: the link between shallow and deep-sea habitats. *Diversity* **12**, 411.

Gianguzza P and Bonaviri C (2013) *Arbacia*. In Miller Lawrence J.(ed). Elsevier, pp. 275-283.

Gray J (1835) On the genera distinguishable in Echinus Lamarck. *Proceedings of the Zoological Society of London* **3**, 57–60.

Gray J (1855) An arrangement of the families of Echinida, with descriptions of some new genera and species. *Proceedings of the Zoological Society of London* **23**, 35–39.

Gregory J (1900) The Echinoderma. In *A Treatise on Zoology*, Lankester, E.R, pp. 237–281. Adam & Charles Black, London.

Haye PA, Segovia NI, Muñoz-Herrera NC, Gálvez FE, Martínez A, Meynard A, Pardo-Gandarillas MC, Poulin E and Faugeron S (2014) Phylogeographic Structure in Benthic Marine Invertebrates of the Southeast Pacific Coast of Chile with Differing Dispersal Potential. *PLOS ONE* **9**, e88613.

Hill SK and Lawrence JM (2003) Habitats and Characteristics of the Sea Urchins *Lytechinus variegatus* and *Arbacia punctulata* (Echinodermata) on the Florida Gulf-Coast Shelf. *Marine Ecology* **24**, 15-30.

Hinderstein LM, Marr JCA, Martinez FA, Dowgiallo MJ, Puglise KA, Pyle RL, ... and Appeldoorn R (2010) Theme section on Mesophotic coral ecosystems: characterization, ecology, and management. *Coral reefs* **29**, 247-251.

Iken K, Brey T, Wand U, Voigt J and Junghans P (2001) Food web structure of the benthic community at the Porcupine Abyssal Plain (NE Atlantic): a stable isotope analysis. *Progress in Oceanography* **50**, 383-405.

Jackson RT (1912) Phylogeny of the Echini: with a revision of palaeozoic species. *Memoirs of the Boston Society of Natural History* 7, 1–491.

Kahng SE, Garcia-Sais JR, Spalding HL, Brokovich E, Wagner D, Weil E and Toonen RJ (2010) Community ecology of mesophotic coral reef ecosystems. *Coral Reefs* **29**, 255-275.

Klein JT (1778) Naturalis Dispositio Echinodermatum. Accessit Lucubratiuncula de Aculeis Echinorum Marinorum et Specilegium de Belemnitis. Edita et Descriptionibus Novisque Inventis et Synonymis Auctorum Auca a Nathanaele Godofredo Leske. Officina Gleditdchiana, Lipsiae (Leipzig).

Kramer N, Eyal G, Tamir R and Loya Y (2019) Upper mesophotic depths in the coral reefs of Eilat, Red Sea, offer suitable refuge grounds for coral settlement. *Scientific Reports* **9**, 1-12.

Koehler R (1914) *Echinoderma I*. Hamburg: Friederichsen and Co.

Lamarck J (1816) Histoire Naturelle des Animaux sans Vertèbres, présentant les caractères géneraux et particuliers de ces animaux, leur distribution, leur classes, leurs familles, leurs generes, et le citation des principales espèces qui s'y rapportent; précédée d'une Introduction offrant la Détermination des caractères essentiells de l'animal, sa distinction du végétal et des autres corps naturels, enfin, l'Exposition des Principes fondamentaux de la Zoologie. Verdière, Paris.

Larraín A (1975) Los equinoideos regulares fósiles y recientes de Chile. *Gayana Zoología* **35**, 5-189.

Lebrato M, Iglesias-Rodríguez D, Feely RA, Greeley D, Jones DO, Suarez-Bosche N, ... and Alker B (2010) Global contribution of echinoderms to the marine carbon cycle: CaCO3 budget and benthic compartments. *Ecological Monographs* **80**, 441-467.

Lessios HA, Lockhart S, Collin R, Sotil G, Sanchez-Jerez P, Zigler KS, ... and Kessing BD (2012) Phylogeography and bindin evolution in *Arbacia*, a sea urchin genus with an unusual distribution. *Molecular Ecology* **21**, 130-144.

Linné CV (1758) *Systema naturae. Tomus I, Regnum animale. Holmiae: Laurentii Salvii.*

Lovén S (1874) Études sur les Échinoïdées. *Kongliga Svenska Vetenskaps-Akademiens Handlingar* **11**, 1–91.

Lovén S (1887) *On the species of Echinoidea described by Linnaeus in his work Museum Ludovicae Ulricae*, Vol. 13. Kongl. boktryckeriet.

Luparello C, Ragona D, Asaro DML, Lazzara V, Affranchi F, Arizza V and Vazzana M (2020) Cell-free coelomic fluid extracts of the sea urchin *Arbacia lixula* impair mitochondrial potential and cell cycle distribution and stimulate reactive oxygen species production and autophagic activity in triple-negative MDA-MB231 breast cancer cells. *Journal of Marine Science and Engineering* **8**, 261.

Micael J, Alves MJ, Costa AC and Jones MB (2016) Exploitation and conservation of echinoderms. In *Oceanography and Marine Biology* pp. 203-220. CRC Press.

Millán C, Díaz A, Poulin E, Merino-Yunnissi C and Martínez A (2019) Genetic diversity and demographic history of the endemic Southeastern Pacific sea urchin *Arbacia spatuligera* (Valenciennes 1846). *Gayana,* **83**, 81-92.

Molina GI (1810) *Saggio sulla storia naturale del Chili*. Masi.

Mortensen T (1910) *Echinoidea of the Swedish South Polar Expedition*, Nordenskjöld O. Stockholm: Lithographisches Institut.

Mortensen T (1935) A monograph of the Echinoidea. v II. Bothriocidaroida, Melonechinoida, Lepidocentroida and Stirodonta. C.A. Reitzel, Copenhagen.

Rocha LA, Pinheiro HT, Shepherd B, Papastamatiou YP, Luiz O J, Pyle RL and Bongaerts P (2018) Mesophotic coral ecosystems are threatened and ecologically distinct from shallow water reefs. *Science* **361**, 281-284.

Roma J, Schertenleib K, Ramalhosa P, Gestoso I, Canning-Clode J and Lenz M (2021). Moderately elevated temperatures increase macroalgal food consumption in two sea urchin species from coastal waters of Madeira. *Journal of Experimental Marine Biology and Ecology* **542**, 151603.

Schumacher CF (1817) *Essai d'un nouveau système des habitations des vers testacés : avec XXII planches*, pp. 1–348. À Copenhague: De l'Imprimerie de Mr. le directeur Schultz.

Shreeves K and Richardson D (2006) Mixed-Gas Closed-Circuit Rebreathers: An Overview of Use in Sport Diving and Application to Deep Scientific Diving.

Smith AB (1980) The structure and arrangement of echinoid tubercles. *Philosophical Transactions of the Royal Society of London. B, Biological Sciences* **289**, 1–54.

Spalding MD, Fox HE, Allen GR, Davidson N, Ferdaña ZA, Finlayson M, Halpern BS, Jorge MA, Lombana A, Lourie SA, Martin KD, McManus E, Molnar J, Recchia CA and Robertson J (2007) Marine Ecoregions of the World: A Bioregionalization of Coastal and Shelf Areas. BioScience 57, 573–583.

Valenciennes AM (1846) *Voyage autour du monde sur la fregate La Venus pendant les annees 1836-39. Atlas 4: Zoophytes.*

World Echinoidea Database https://www.marinespecies.org/echinoidea Accessed online 10 October 2022.

Figures

Fig. 1. Map of distribution and records of the sea urchin *Arbacia spatuligera* in shallow (<30 m depth) and mesophotic reefs (36-63 m depth) in the Southeastern Pacific Ocean: The black asterisk represents all previous records in the literature and OBIS.org; (2) the green points represents two locations of the shallow rocky reefs with *Macrocystis pyrifera*; (3) the orange point is a single location of a mesophotic rocky reef covered by turf algae; (4) the yellow point represents a mesophotic sandy slope; and finally (5) the black-flagged points represent two shipwrecks within the mesophotic reef ecosystem.

Fig. 2. Photographic records of *Arbacia spatuligera* and their habitats in three of four mesophotic temperate reefs off Central Coast of Chile: (A-C) individuals recorded on deck and hull of a shipwreck between 36-46 m deep with the presence of filamentous algae and the striped anemone *Anthothoe chilensis*; (D-H) individuals recorded on a sandy slope with plastic debris, abandoned fishing gear, and a car wheel between 40-56 m deep with the presence of filamentous algae and the lobed anemone *Antholoba achates*; (G) aggregation of 10 individuals; (I-O) individuals from the rocky reef between 40-58 m deep with filamentous algae, sponges, crustose algae (order Corallinales), and channels with sand.

Fig. 3. Morphology of *A. spatuligera* from Chile: (A-C), *Arbacia spatuligera* from Pichidangui; (A), aboral view; (B), oral view; (C), lateral view; (D-F), *Arbacia spatuligera* from Las Cruces; (D), aboral view; (E), oral view; (F), lateral view. Scale bar equals 10 mm.

Fig. 4. *Arbacia spatuligera*, details of test plating. A-B, apical system: A, small specimen (TD = 30 mm); B, larger specimen (TD = 45 mm); C, aboral plate of ambulacrum; D-E, aboral plates of interambulacrum: D, small specimen (TD = 30 mm); E, larger specimen (TD = 70 mm). Scale bars equal 10 mm.

Fig. 5. A-D, SEM photographs of valves of pedicellariae of *Arbacia spatuligera*; A, valve of apical ophicephalous pedicellaria; B, valve of oral ophicephalous pedicellaria; C, valve of

apical tridentate pedicellaria; D, valve of apical tridentate pedicellaria. Scale bars equal 300 µm.

Fig. 6. *Arbacia spatuligera* new morphotype recorded off Algarrobo, Chile at 60 m deep. Photo credit: Millenium Nucleus for Ecology and Conservation of Temperate Mesophotic Reef Ecosystem (NUTME) 2023.

Fig. 7. Shallow records of *Arbacia spatuligera* in two rocky reefs in the Biobio Region, Chile: (A-B) Laraquete; (C-D) Penco.

Table I. Localities surveyed with the sampling year, geographical coordinates, country, reef type, habitat (**RRWM:** Rocky reef with *Macrocystis pyrifera*; **SWCK:** Shipwreck; **RRWCA:** Rocky reef with calcareous algae; **SSWD:** Sandy slope with debris), depth range, number of organisms, survey technique (**VC**: Visual census; **C:** Collected) diving system, and references.

Year	Location	Longitude	Latitude	Country	Reef type	Habitat	Depth range (m)	# organisms	Survey technique	Diving System	Reference
1999	Islas Lobos de Afuera	-80,7083	-6,925	Peru	Shallow	N/A	20	>50	VC	Hookah (air)	Hooker et al., 2005
2018	Lima	-77,2464	-11,9883	Peru	Shallow	N/A	10-30	17	C	Open circuit (air)	Millán et al., 2019
2018	Arica	-70,3217	-18,4531	Chile	Shallow	N/A	10-30	18	C	Open circuit (air)	Millán et al., 2019
2016	Taltal	-70,5158	-25,3897	Chile	Shallow	N/A	10-30	29	C	Open circuit (air)	Millán et al., 2019
2016	Coquimbo	-71,3531	-29,9639	Chile	Shallow	N/A	10-30	46	C	Open circuit (air)	Millán et al., 2019
2022	Pichidangui	-71,541	-32,1325	Chile	Mesophotic	RRWCA	40-58	80	VC	CCR (trimix)	This work
2022	Valparaíso	-71,6288	-33,0217	Chile	Mesophotic	SSWD	40-56	23	VC	CCR (trimix)	This work
2019	Valparaíso	-71,6188	-33,0337	Chile	Mesophotic	SWCK	58-63	10	VC	CCR (trimix)	This work
2022	Valparaíso	-71,6092	-33,0359	Chile	Mesophotic	SWCK	36-46	15	VC	CCR (air)	This work
N/A	Faro Cabo Carranza	-72,7	-35,5667	Chile	Shallow	N/A	NA	N/A	C	N/A	David et al., 2005
N/A	Los Morros	-73	-36,5333	Chile	Shallow	N/A	NA	N/A	C	N/A	David et al., 2005
N/A	Costa Larga	-73,1	-36,6667	Chile	Shallow	N/A	NA	N/A	C	N/A	David et al., 2005
2021	Penco	-72,9963	-36,7292	Chile	Shallow	RRWM	5,1	220	VC	Open Circuit (air)	This work
2016	Concepción	-73,1703	-36,7603	Chile	Shallow	N/A	10-30	30	C	Open circuit (air)	Millán et al., 2019
2021	Laraquete	-73,1735	-37,1411	Chile	Shallow	RRWM	7,4	188	VC	Open Circuit (air)	This work

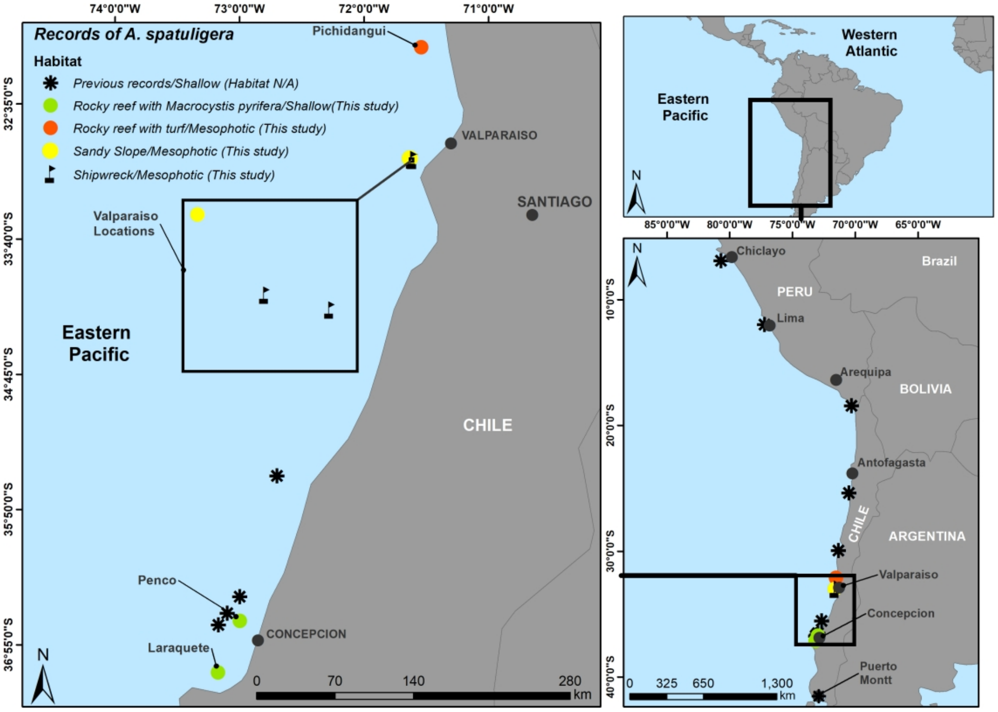

Fig. 1. Map of distribution and records of the sea urchin Arbacia spatuligera in shallow (<30 m depth) and mesophotic reefs (36-63 m depth) in the Southeastern Pacific Ocean: The black asterisk represents all previous records in the literature and OBIS.org; (2) the green points represents two locations of the shallow rocky reefs with Macrocystis pyrifera; (3) the orange point is a single location of a mesophotic rocky reef covered by turf algae; (4) the yellow point represents a mesophotic sandy slope; and finally (5) the black-flagged points represent two shipwrecks within the mesophotic reef ecosystem.

297x210mm (300 x 300 DPI)

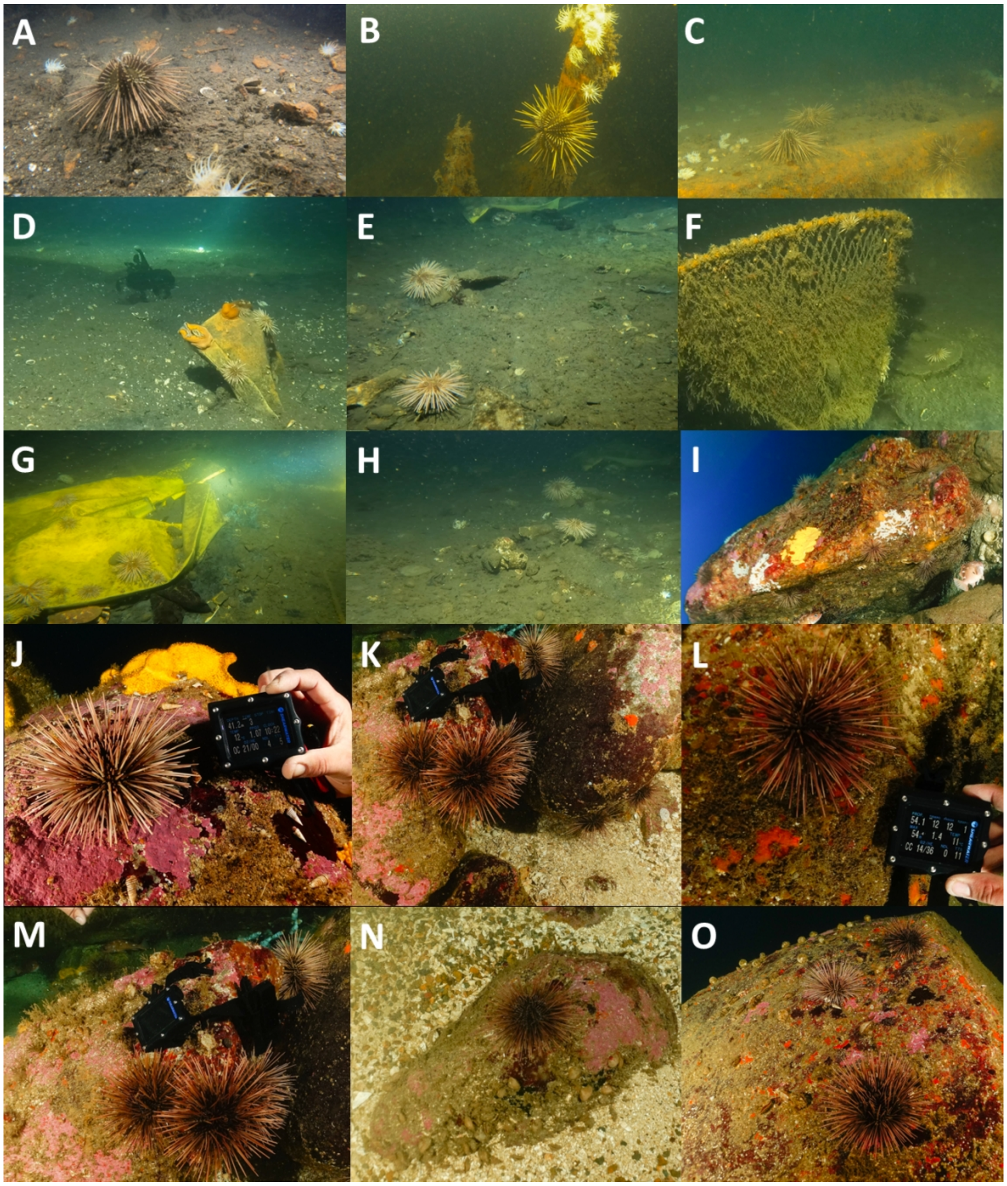

Fig. 2. Photographic records of Arbacia spatuligera and their habitats in three of four mesophotic temperate reefs off Central Coast of Chile: (A-C) individuals recorded on deck and hull of a shipwreck between 36-46 m deep with the presence of filamentous algae and the striped anemone Anthothoe chilensis; (D-H) individuals recorded on a sandy slope with plastic debris, abandoned fishing gear, and a car wheel between 40-56 m deep with the presence of filamentous algae and the lobed anemone Antholoba achates; (G) aggregation of 10 individuals; (I-O) individuals from the rocky reef between 40-58 m deep with filamentous algae, sponges, crustose algae (order Corallinales), and channels with sand.

112x131mm (300 x 300 DPI)

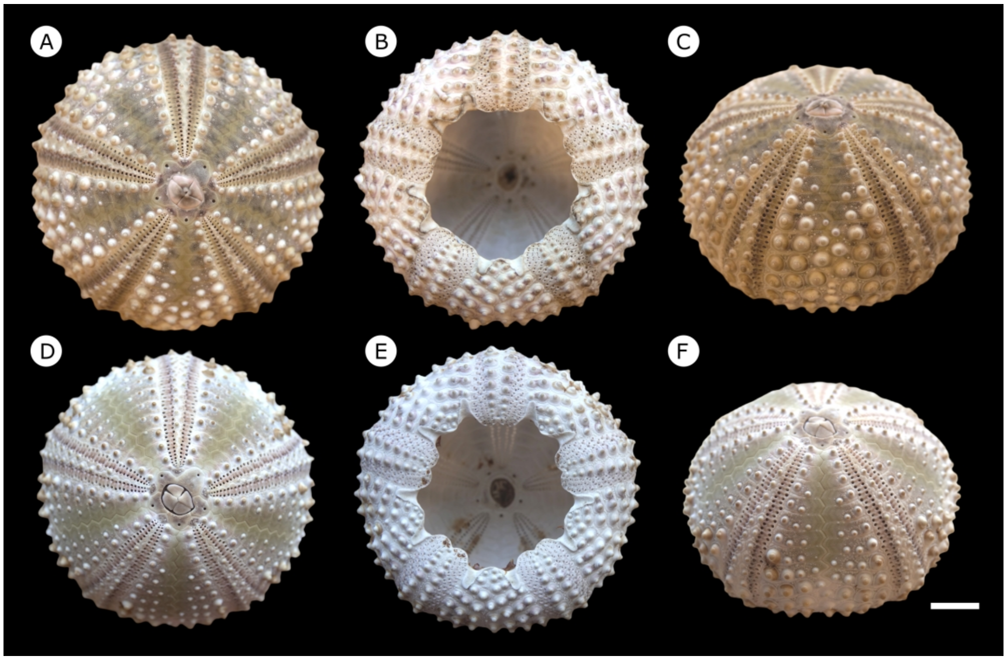

Fig. 3. Morphology of A. spatuligera from Chile: (A-C), Arbacia spatuligera from Pichidangui; (A), aboral view; (B), oral view; (C), lateral view; (D-F), Arbacia spatuligera from Las Cruces; (D), aboral view; (E), oral view; (F), lateral view. Scale bar equals 10 mm.

200x130mm (300 x 300 DPI)

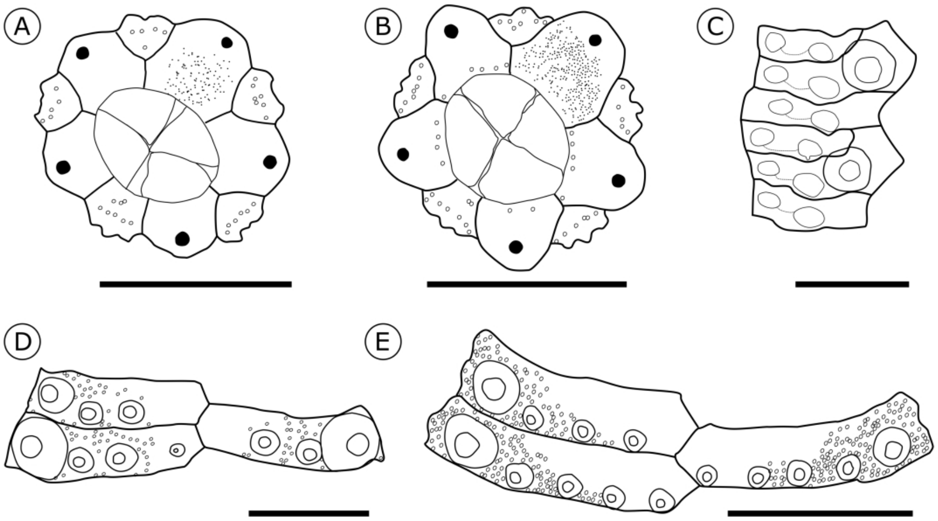

Fig. 4. Arbacia spatuligera, details of test plating. A-B, apical system: A, small specimen (TD = 30 mm); B, larger specimen (TD = 45 mm); C, aboral plate of ambulacrum; D-E, aboral plates of interambulacrum: D, small specimen (TD = 30 mm); E, larger specimen (TD = 70 mm). Scale bars equal 10 mm.

169x94mm (600 x 600 DPI)

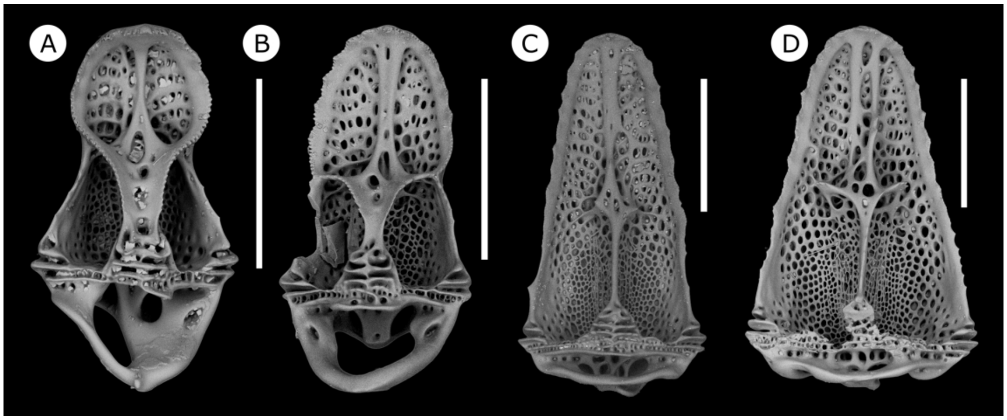

Fig. 5. A-D, SEM photographs of valves of pedicellariae of Arbacia spatuligera; A, valve of apical ophicephalous pedicellaria; B, valve of oral ophicephalous pedicellaria; C, valve of apical tridentate pedicellaria; D, valve of apical tridentate pedicellaria. Scale bars equal 300 µm.

170x70mm (300 x 300 DPI)

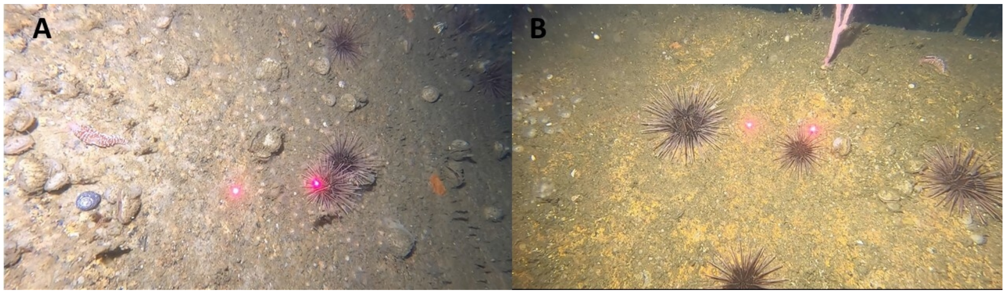

Fig. 6. Arbacia spatuligera new morphotype recorded off Algarrobo, Chile at 60 m deep. Photo credit: Millenium Nucleus for Ecology and Conservation of Temperate Mesophotic Reef Ecosystem (NUTME) 2023.

108x31mm (300 x 300 DPI)

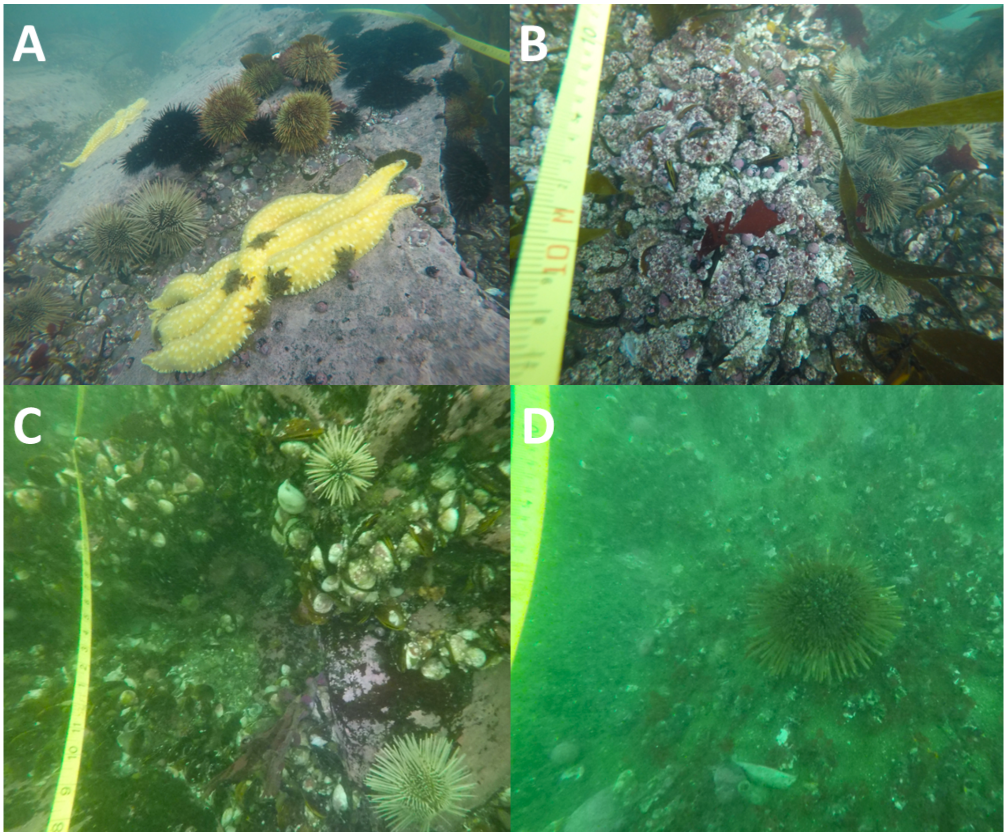

Fig. 7. Shallow records of Arbacia spatuligera in two rocky reefs in the Biobio Region, Chile: (A-B) Laraquete; (C-D) Penco.

96x79mm (300 x 300 DPI)